Applied Geochemistry 122 (2020) 104713

Contents lists available at ScienceDirect

Applied Geochemistry

journal homepage: http://www.elsevier.com/locate/apgeochem

Comparative study of radium and strontium behaviour in contact with cementitious materials

Jana Kittnerová [a,*], Barbora Drtinová [a], Karel Štamberg [a], Dušan Vopálka [a], Nicholas Evans [b], Guido Deissmann [c], Steve Lange [c]

[a] Czech Technical University in Prague, Břehová 7, 115 19, Prague 1, Czech Republic
[b] Centre for Environment Fisheries and Aquaculture Science, Pakefield Rd, Lowestoft, Suffolk, NR33 0HT, United Kingdom
[c] Institute of Energy and Climate Research (IEK-6), Nuclear Waste Management and Reactor Safety, Forschungszentrum Jülich GmbH, 52425, Jülich, Germany

ARTICLE INFO

Editorial handling by Prof. M. Kersten

Keywords:
Radium
Strontium
Sorption
Distribution ratio
Isotherm
Activation energy

ABSTRACT

A comparative study of the sorption behaviour of radium and strontium was performed on various cementitious materials including crushed hardened cement pastes (HCP) and concretes as well as a synthesised calcium silicate hydrate (CSH) phase.

R_d values obtained for the Ra and Sr uptake on commercial cement materials were in the range of 50–380 L kg^{-1} and 10–30 L kg^{-1}, respectively. No significant difference between the distribution ratios of the isotopes ^{226}Ra and ^{223}Ra was observed in the studied liquid to solid (L/S) ratio range, although different isotherms were determined. The R_d values for Ra were found to increase with increasing L/S ratio. The cause of this effect is obviously the non-linearity of the sorption isotherm, here of the convex type. In contrast, Sr uptake seemed to be largely unaffected by variation of L/S ratios; this indicates an isotherm of almost linear type. Sorption experiments with the CSH phase confirmed the distinctive differences in the sorption behaviour between Ra and Sr as expected, with R_d values significantly higher for Ra. Similarly, the difference between real cementitious materials and the pure CSH phase was confirmed, indicating that the sorption of alkaline earth elements is mainly due to uptake by CSH.

The kinetics of Ra and Sr uptake on cementitious materials were evaluated by a set of models describing the sorption in heterogeneous systems based on different rate-controlling processes. The FD (film diffusion) model in the case of Ra, and the ID (diffusion in inert layer) model in the case of Sr provided the best fits.

The influence of temperature on the kinetics of radium sorption was studied, suggesting change in the shape of isotherm with increasing temperature. Evaluation of sorption kinetic data yielded values of the apparent activation energy of the uptake process.

Complementary through diffusion experiments using compacted crushed HCP confirmed and extended the findings obtained by evaluation of the batch sorption experiments performed with Ra and Sr.

1. Introduction

Cementitious materials are planned to be used as a structural support in deep geological repositories for radioactive waste, and, depending on the repository concept, for backfilling and/or waste conditioning or as a component in waste containers (Jantzen et al., 2010; Lagerblad, 2001). According to the Swedish repository safety case (SKB, 2011) and with respect to the direct disposal of spent nuclear fuels, ^{226}Ra can be a one of the most important contributors to dose in the long term (i.e. after more than 100,000 years) due to the large amount of uranium present within the waste inventories, as ^{226}Ra is a long-lived radionuclide originating from the decay of ^{238}U.

In addition, a significant part of low and intermediate level radioactive waste containing radium is stored in the Czech Republic in the Bratrství repository that will be sealed in the near future. As barriers in this repository are based on cementitious materials and ^{226}Ra is one of the main contaminants of interest, SURAO (the Czech Radioactive Waste Repository Authority) has decided to study the behaviour of radium in hydrated cement material systems.

^{90}Sr is an important fission product of ^{235}U in nuclear reactors with a

* Corresponding author.
E-mail address: Jana.Kittnerova@fjfi.cvut.cz (J. Kittnerová).

https://doi.org/10.1016/j.apgeochem.2020.104713
Received 14 October 2019; Received in revised form 23 July 2020; Accepted 24 July 2020
Available online 5 August 2020

half-life of 28.8 years. Moreover, strontium is often considered as an analogue of radium, as these two elements are chemically similar (Berner, 2003; Tits et al., 2006b).

For the assessment of the long-term safety of a repository, the retardation mechanisms of radionuclides on cementitious materials within the engineered barriers need to be understood. The interaction of a radionuclide with cementitious materials depends on the type of radionuclide and also on the type of cement. The sorption of radionuclides (electrostatic sorption, chemisorption and adsorption) and substitution (e.g. Sr for Ca) are processes influencing radionuclide retardation in the presence of cementitious materials (Atkins and Glasser, 1992; Evans, 2008; Jantzen et al., 2010). It should be added that the capture of contaminants can also occur by surface complexation mechanisms and ion exchange, especially when the solid phases have a silicate or aluminate-silicate structure – see database RES^{3}T (Brendler, 2006) or the monography of Lützenkirchen (2006).

The mobility of Ra in cementitious systems is controlled by the solubility of Ra-bearing phases under highly alkaline conditions, diffusion, interface processes, or incorporation into solid phases. For long-term modelling studies on radionuclide migration (e.g. Piqué et al., 2013), knowledge about the retardation mechanism, as well as of the kinetics and strength of radionuclide uptake for a given cementitious material are required. The composition of hydrated cementitious materials can vary significantly between different types of cements, thus affecting the sorption behaviour of radionuclides. For phenomenological sorption studies, it is possible to use commercial cement materials such as hardened cement pastes (HCP) or concretes, in particular those intended for use in a repository system. Moreover, studies on individual hydration phases that occur in cementitious materials can provide further insights into the radionuclide retention mechanisms. These phases are for example calcium silicate hydrates (CSH) with variable composition, ettringite (AFt, $Ca_6Al_2(SO_4)_3(OH)_{12}{\cdot}26H_2O$) or the hydrocalumite-like AFm ($Ca_4Al_2(OH)_{12}$ (X^{2-})$\cdot 6H_2O$, where X refers to e.g. $2Cl^-$, SO_4^{2-} etc.). By comparing the sorption properties of these phases (see e.g. Lange et al., 2018), the predominance of cation sorption to CSH is evident and therefore this material has been chosen in this study. The complex structure of CSH changes with both time and composition (Chen et al., 2004; Nonat, 2004), which affects the radionuclide sorption that is also influenced by various other factors such as calcium to silicon (C/S) ratio of the CSH or pore water pH (Lange et al., 2018).

The current state of knowledge of distribution ratios of Ra on commercial cements is based on rather few studies. For example, Tits et al. (2006a) determined the distribution coefficients of ^{226}Ra (with initial concentration about 10^{-8} mol L^{-1}) to be 140 L kg^{-1} for degraded HCP (type CEM I) and up to 400 L kg^{-1} for fresh HCP. Bayliss et al. (1989) obtained R_d's for radium (concentration about 10^{-8}–10^{-11} mol L^{-1}) for sulphate resistant Portland cement (SRPC) and ordinary Portland cement blended with blast furnace slag (OPC:BFS) in the range of 50–500 L kg^{-1} for SRPC and 850–1800 L kg^{-1} for OPC:BFS. R_d for Ra in the study of Holland and Lee (1992) was measured to be 50 L kg^{-1} for OPC, whereas for tobermorite (crystalline form of CSH) R_d's were in the range 10^4–10^5 L kg^{-1}. Recent studies (Lange et al., 2018; Olmeda et al., 2019) confirm previous knowledge. Lange et al. (2018) describe sorption of ^{226}Ra onto HCP CEM I (OPC) with R_d values up to 100 L kg^{-1}, Olmeda et al. (2019) presents result for ^{226}Ra sorption on HCP CEM V (containing blast furnace slag and fly ash) for fresh and degraded state of HCP as $R_d \approx 590$ L kg^{-1} and 490 L kg^{-1}, respectively. Both studies compare R_d's obtained for HCP with data obtained on CSH with different C/S ratios. As mentioned in e.g. Richardson (2008), addition of admixtures to OPC decreases the C/S ratio of CSH in HCP and thus increases R_d values of cationic radionuclide (e.g. Ra), which is consistent with the increase of R_d's with lower C/S ratios in CSH sorption experiments (Lange et al., 2018; Olmeda et al., 2019; Tits et al., 2006a).

In comparison, R_d for strontium on HCP of type CEM II (slightly different material than HCP CEM II used in this work) was determined to be in the range 12–22 L kg^{-1} in previous research. According to Li and Pang (2014) and Ochs et al. (2016), who compared Sr sorption studies on a variety of cementitious materials, R_d achieved maximum values of 100 L kg^{-1}.

As expected, the distribution ratios of radium and strontium on pure CSH are higher compared to commercial cement materials. Sorption experiments with Ra are quite rare, but in Tits et al. (2006a) the range of distribution ratios of Ra for the pure CSH phases was determined in the order of 10^2–10^4 L kg^{-1} depending on C/S ratio, where the lower C/S means higher R_d values. Lange et al. (2018) and Olmeda et al. (2019) describe the same tendency of increasing R_d's of radium sorption on CSH with lower C/S ratio. Olmeda et al. (2019) presents R_d in the range of 560–14800 L kg^{-1} within the C/S ratio 1.6–0.8. Lange et al. (2018) compares R_d's of ^{226}Ra for CSH with C/S ratio 0.9 and 1.4, the results are in orders of 10^4 and 10^3 L kg^{-1}, respectively. R_d of Sr for CSH was determined in several studies (Iwaida et al., 2000; Tits et al., 2006b), where the R_d values are also affected by the C/S ratio in CSH – from these dependencies, the R_d values for C/S = 1.4 can be estimated as about 100 L kg^{-1}.

The aim of this study was to investigate the equilibrium R_d values and kinetic dependencies of the sorption of radium and strontium on selected types of cementitious materials used for radioactive waste management in the Czech Republic. It means, to take a closer look at the analogy of Ra and Sr from the point of view of their uptake under various conditions, including the investigation of the effect of temperature on radionuclide sorption. Also, the distribution ratios of two isotopes of radium were compared to determine the possibility to use ^{223}Ra instead of ^{226}Ra in research, since working with ^{223}Ra is considerably safer than with ^{226}Ra because of their daughters' half-lives. Finally, complementary diffusion experiments with ^{223}Ra and ^{85}Sr using compacted HCP CEM II were performed to extent the sorption studies to more realistic L/S ratios.

2. Materials and methods

2.1. Cementitious materials

A comparative study of the sorption behaviour of Ra and Sr was performed on several cementitious materials: three hardened cement pastes (HCP CEM I, CEM II, and CEM III) and two types of concrete made from the same cements as two of the HCP's used (C CEM I and C CEM III). Both concretes have actually been used in the low/intermediate level waste (LLW-ILW) repositories in the Czech Republic. The designation of the cements corresponds to the European cement standard EN 197, where CEM I is ordinary Portland cement, CEM II Portland cement with another constituent (here CEM II/A-S which contains a blast furnace slag) and CEM III refers to blast furnace slag cement. Concretes were made from cements (17% in case of C CEM I and 19% in C CEM III) with the addition of aggregates, fly ash and plasticizers. All materials (age of the material in the range of 1–3 years) were crushed and sieved to a fraction ≤ 0.4 mm prior to use in sorption and diffusion experiments.

Besides these commercially available commonly used cements, a synthetic cement hydration phase was studied: calcium silicate hydrate (CSH) with C/S = 1.4, prepared following the procedure of Atkins et al. (1992) and described in detail in Lange et al. (2018).

2.2. Radionuclides

The isotopes of interest, i.e. ^{226}Ra and ^{90}Sr were used for sorption studies on CSH. To aid detection, ^{223}Ra and ^{85}Sr were used as substitutes for ^{226}Ra and ^{90}Sr, respectively, in most experiments in the sorption studies on commercial cement materials. ^{223}Ra is predominantly an α-emitter (half-life = 11.43 days) that decays to ^{219}Rn with a final decay product of ^{207}Pb (Collins et al., 2015). The radon isotope ^{219}Rn has a half-life of only 4 s. The advantage of the much shorter half-life of ^{219}Rn compared to ^{222}Rn is that it is much safer to work with. The isotope

^{223}Ra (commonly used in radiotherapy) was obtained from a ^{227}Ac/^{223}Ra generator consisting of a glass column filled with Dowex-1 × 8 resin. Elution of ^{223}Ra was carried out with 0.7 mol L^{-1} nitric acid in 80% methanol. The eluate was evaporated to dryness in a vacuum evaporator and then dissolved in 1 mol L^{-1} nitric acid (Kozempel et al., 2015). In the case of Sr, the isotope ^{85}Sr (as Sr-chloride) in 0.5 mol L^{-1} hydrochloric acid was used either with ($c_0 = 3.5 \cdot 10^{-4}$ mol L^{-1} $SrCl_2$) or without carrier.

2.3. X-ray diffraction analysis

The powdered materials were characterized prior to the uptake studies by X-ray diffraction analysis in Θ-2Θ Bragg-Brentano geometry using a Rigaku MiniFlex 600 diffractometer equipped with a Cu X-ray tube (average wavelength $K_{\alpha 1,2} = 0.15418$ nm). High voltage and current settings used were 40 kV and 15 mA, respectively. The measurements were performed in continuous mode in the range of 2Θ = 10°–80° with a collection speed of 2°/min. The measured range was divided into intervals for data collection with the width equal to 0.02°. The evaluation was performed using the PDXL2 program and the ICDD PDF-2 database (version 2013).

2.4. Sorption experiments – commercial cements

Distribution ratios and sorption kinetics were measured for ^{223}Ra and ^{85}Sr for HCP CEM II, C CEM I and C CEM III over a period of 4 days (96 h). The kinetic experiments were carried out to establish the appropriate time for the duration of equilibrium experiments for the determination of R_d values as well as for evaluation with kinetic models. It was confirmed that the time of 96 h, in terms of achieving virtually zero concentration changes, was sufficient to achieve an equilibrium, or close-to-equilibrium state of the sorption of ^{223}Ra and ^{85}Sr under the given laboratory conditions. The same duration was also estimated to be suitable for HCP CEM I and HCP CEM III with respect to comparison with the results obtained for HCP CEM II, C CEM I and C CEM III.

The experiments were carried out under ambient conditions, however, all containers (polypropylene ampoule with maximum working volume of 12 mL) were carefully sealed with parafilm. Both the kinetic and distribution ratio studies of Ra and Sr uptake were conducted with simulated cementitious pore water, which was a saturated solution of portlandite ($Ca(OH)_2$, pH = 12.4–12.6). The experiments were performed at liquid to solid ratios (L/S) of 10–600 L kg^{-1} (6 mL of liquid phase) at temperatures ranging from 22 to 80 °C as the temperature in geological repository can be significantly higher than the average room temperature. The kinetic experiments were interrupted at predetermined intervals (2, 4.5, 8, 24, 30, 48 and 96 h) for sampling: 2 mL of the centrifuged liquid phase were taken and analysed for the radionuclide activity using a well-type NaI(Tl) scintillation detector. The samples were then returned to the reaction vial, so the ratio of the phases remained at the original value during the experiment. The equilibrium experiments were handled similarly to the kinetic experiments after an equilibration time of 96 h.

Carrier-free ^{223}Ra was used, which corresponds to a concentration of about 10^{-12} mol L^{-1}. According to calculations performed by Berner (2003), the maximum concentration of Ra in cementitious pore water (pH 12.55, 25 °C) would be given by a solubility limit of about $1 \cdot 10^{-5}$ mol L^{-1} (depending on the concentration of free SO_4^{2-}). In the system with presence of CO_2 (or CO_3^{2-} respectively) it is calculated approx. as $1 \cdot 10^{-4}$ mol L^{-1}. As far as CO_3^{2-} is concerned, this, due to the low solubility of $CaCO_3$, is limited by a Ca^{2+} concentration which should not exceed $1 \cdot 10^{-4}$ mol L^{-1}. On the other hand, ^{85}Sr was used with a carrier – $SrCl_2$ at a concentration of $3.5 \cdot 10^{-4}$ mol L^{-1}. This Sr concentration corresponds to the concentration of stable Sr that was determined by leaching the HCP CEM II in distilled water for 1 month at L/S = 5 L kg^{-1}. A comparative experiment with Sr in a carrier-free scenario was performed to determine the effect of the carrier. It must be pointed out that commercial cements naturally contain strontium and radium (mainly ^{226}Ra). The possible content of ^{226}Ra in commercial cements was determined in the leachates by gamma measurement with a coaxial HPGe detector (Princeton Gamma Technologies) with multichannel analyser Ortec 919 Spectrum Master and Maestro software, but the content of ^{226}Ra in measured samples was not separable from the background.

Due to the relatively short half-life of ^{223}Ra, the observed decrease of radioactivity in the liquid phase caused by the uptake of the radionuclide on the solid cementitious material had to be decay corrected. For this correction a procedure based on exponential decay was used to convert all measured data (Eq. (1)) to the same time point t_0 corresponding to the start of the experiment.

Prior to the sorption measurements on commercial cement materials, their moisture content (approx. 10%) was determined and taken into account during evaluation. Furthermore, the sorption on the walls of the experimental polypropylene vial was determined across all conditions. For Ra, sorption to vial walls was set at 7.8%, for Sr at 5.8%; these findings were included during evaluation of the experiments.

^{226}Ra sorption experiments on HCP and concrete based on commercial cements (i.e. HCP CEM I, HCP CEM II, C CEM I, C CEM III) were also performed to assess the suitability of the use of ^{223}Ra instead of ^{226}Ra. The duration of experiments with ^{226}Ra at room temperature was three weeks (500 h), the starting working solution was a leachate from HCP CEM I. The L/S ratio in the sorption experiments was chosen to be 25, 100 and 200 L kg^{-1}, the concentration of ^{226}Ra was $5 \cdot 10^{-7}$ mol L^{-1}. The long half-life of ^{226}Ra (1600 years) eliminates possible uncertainties caused by the radioactive decay as in the case of the short-lived ^{223}Ra isotope. Gamma measurement of ^{226}Ra in filtered liquid samples was done by using a coaxial N type detector system (type: EGC 35-195-R), purchased from Eurisys Mesures, Lingolsheim, France, equipped with a spectrometer system obtained from EG & G Ortec Munich, Germany. Analyses of the spectra were performed with the GammaVision® Modell A66-B32 software (version 5.20).

The uptake of the radionuclides by the cementitious materials is characterized in terms of the distribution ratio, R_d, between liquid and solid phases calculated according to Eq. (1)

$$R_d = \frac{A_{init} - A_t}{A_t} \cdot \frac{V}{m}, \quad (1)$$

where A_{init} (Bq) is the initial activity concentration of the radionuclide in solution in the unit of activity and A_t corresponds to the activity concentration at time t, respectively, V (L) is the volume of the liquid phase and m (kg) the mass of solid phase used in the experiment. Molar concentrations, c (mol L^{-1}), in the liquid phase were calculated using Eq. (2)

$$c = \frac{A \cdot T_{1/2}}{ln\ 2 \cdot V \cdot N_A}, \quad (2)$$

where A (Bq) is absolute activity of the radionuclide, $T_{1/2}$ (s) is radionuclide half-life, V (L) is volume of the solution and N_A is Avogadro constant ($6.022 \cdot 10^{23}$ mol^{-1}).

2.5. Sorption experiments – CSH

Sorption experiments on synthetic CSH (C/S = 1.4) were performed as similar as possible to those for sorption on HPC and concrete. However, the CSH experiments were held under an inert gas atmosphere of argon in a glove-box, as the CSH is more sensitive to CO_2 than HCP or concrete. Two radionuclides were used for these experiments: ^{226}Ra, and ^{90}Sr. Radionuclide sorption experiments were carried out in saturated CSH solution at an L/S ratio of 200 L kg^{-1} using initial Ra and Sr concentrations in the range $5 \cdot 10^{-10}$–$8 \cdot 10^{-7}$ mol L^{-1}, which were achieved in the cases of Sr by the addition of a carrier ($Sr(OH)_2$). The sorption studies were performed at room temperature and lasted for three weeks (approx. 500 h). ^{226}Ra in the filtrated liquid phase was measured by

gamma spectroscopy on an HPGe detector (as described above), for ^{90}Sr liquid scintillation counting (LSC) was used (1220 Quantulus, PerkinElmer, Winq software version 1.2).

2.6. Kinetic models for two-phase (liquid-solid) systems

The kinetics of the sorption experiments were evaluated via several kinetics models with the aim of assessing the type of prevailing rate-controlling processes for the systems studied. These kinetic models, summarized in Table 1, reflect the following rate-controlling processes: mass transfer, or two-film model (DM), film diffusion (FD), diffusion in inert layer (ID) and chemical reaction (CR). In addition, two other kinetic models were derived, namely, diffusion in reacted layer (RLD) and gel diffusion (GD). However, these models were omitted here due to the character of the solid phase, which is neither reacted nor gel-like. Detailed derivation of FD, ID, CR, RLD and GD models can be found in (Štamberg and Cabicar, 1980) and DM in monograph Mass Transfer Operations (Treybal, 1956). To derive the FD, ID, CR and RLD models, the principles used in a case of the so-called Ash model (Levenspiel, 1962) were applied.

In Table 1 c is a concentration of the component in the aqueous phase at time t; q – concentration of the component in the sorbent at time t; c^* – equilibrium concentration of the component in the aqueous phase corresponding to the equilibrium concentration q^* of the component in the sorbent; q_0 – starting concentration of the component in the sorbent; t – time; r (L/S) – ratio of aqueous to solid phase; D – diffusion coefficient of the component, K_{DM}; K_{FD}, K_{ID}, K_{CR}, – over-all kinetic coefficients; k_{CR} – kinetic coefficient of the chemical reaction; r_{CR} – rate of the chemical reaction; R – mean radius of the solid phase particle; ρ – density of the solid sorbent; δ – thickness of the "liquid film" on the surface of the solid particle.

The experimentally measured decreasing concentrations in the liquid phase, $-dc/dt$, were compared to the concentrations computed by the individual kinetic models (after each experimental time-step). A fourth-order Runge-Kutta method was used for the numerical solution of differential equation selected from Table 1; the Newton-Raphson non-linear regression method was used for the determination of desired parameter of the given kinetic model, e.g. K_{FD}, by minimizing the value of the goodness-of-fit parameter. The quantity $\frac{\chi 2}{\nu}$ (or $\frac{WSOS}{DF}$, see Eq. (3)) is believed to be the appropriate parameter for the goodness-of-fit, it holds that the fit is acceptable if $0.1 < \frac{WSOS}{DF} < 20$ (Herbelin and Westall, 1996).

$$\chi 2 = \sum_{i}^{n} \frac{SSx_i}{s_i^2} \tag{3}$$

Here SSx_i is the square of the i-th deviation of the corresponding experimental value from the calculated one, s_i is an estimate of the standard deviation of the i-th experimental point, and degree of freedom, ν (or DF), is the number of experimental points (n) reduced by the number of independent parameters (n_p). In the evaluation of the kinetic experiments, it was assumed that the relative standard deviation of all experimental uptake data is 0.1 and that the results of long-term experiments determine the shape of the equilibrium isotherm. This approach to the evaluation of kinetic sorption experiments was already successfully applied in some other works, for example, to describe the kinetics of radionuclide sorption on natural materials (e.g. Beneš et al., 1994; Lujaniene et al., 2012), and ion exchangers (e.g. Helfferich, 1959; Štamberg and Cabicar, 1980), or liquid-liquid extraction (Distler et al., 2020, 2018). To evaluate kinetics, it is necessary to determine the parameters of the sorption isotherms, in this case Langmuir or Freundlich ones, whose general formulae are given in Table 1. Experimental data obtained at different phase ratios, L/S, after 96 h were used to determine isotherm parameters.

Table 1
Kinetic models of sorption in two-phase systems used for the evaluation of sorption kinetics in systems with crushed cementitious material in an alkaline working solution.

Controlling process	Model notation	Differential equation
Mass transfer	DM	$\frac{dq}{dt} = K_{DM}(q^* - q)$
Film diffusion	FD	$\frac{dq}{dt} = K_{FD}(c - c^*)$; $K_{FD} = \frac{3D}{\delta R\rho}$
Diffusion in an inert layer	ID	$\frac{dq}{dt} = K_{ID}\frac{c - c^*}{\left(1 - \frac{q}{q^*}\right)^{-\frac{1}{3}} - 1}$; $K_{ID} = \frac{3D}{R^2\rho}$
Chemical reaction (taking place in the reaction zone, here for the first order reversible reaction)	CR	$\frac{dq}{dt} = K_{CR}\frac{(c - c^*)}{\left(1 - \frac{q}{q^*}\right)^{-\frac{2}{3}}}$; $K_{CR} = \frac{3k_{CR}}{R\rho}$; $r_{CR} = k_{CR}(c - c^*)$

Following equations hold: $dq/dt = -r \cdot dc/dt$
if c is the integration variable: $q = r\,(c_0 - c) + q_0$
if q is the integration variable: $c = c_0 - (q - q_0)/r$
Langmuir equilibrium equations used: $q^* = (K_L{\cdot}c{\cdot}Q)/(1{+}K_L{\cdot}c)$ and $c^* = q/(K_L \cdot (Q - q))$
Freundlich equilibrium equations used: $q^* = K_F \cdot c^p$, and $c^* = (q/K_F)^{1/p}$

2.7. Diffusion experiments

Through diffusion experiments with ^{223}Ra ($c_0 \approx 10^{-12}$ mol L^{-1}) and ^{85}Sr ($c_0 = 3.5{\cdot}10^{-4}$ mol L^{-1} with $SrCl_2$ carrier) were carried out in a saturated $Ca(OH)_2$ solution using compacted HCP CEM II layers as porous media, which were obtained by pressing the crushed HCP (experimental set-up described in detail in Gondolli and Večerník (2014); cf. Fig. 1). The layer of cementitious material (width 0.5 cm, diameter 3 cm) was saturated with the working solution prior to the addition of the migrating species in the inlet container. The volumes of the inlet and outlet containers (polycarbonate glass) were 50 mL. Separating filters (CrNi(Mo) steel) of 0.08 cm width and a pore size of about 10 μm were used for the separation of the cementitious material from the containers with working solutions. The duration of the experiments was 22 days, due to the relatively short half-life of the ^{223}Ra isotope. The aim of these experiments was the extension of the study of the influence of phase ratio L/S on the distribution ratio, since the L/S ratio in the diffusion cell differs significantly from the L/S ratio used in sorption experiments. During the duration of the experiment, 2 mL of samples of inlet and outlet solutions were withdrawn in regular intervals and measured using a well-type NaI(Tl) scintillation detector. After the measurement the samples were returned into the reservoirs. After the termination of the experiment, the cement layer was cut into the thin slices of 0.5 mm. Each slice was placed into a measuring vial, weighed, measured on a NaI(Tl) detector (with addition of 2 mL of distilled water to maintain homogeneous geometry), dried in an air dryer and then weighed again to determine the water content in all sliced samples.

For the evaluation of the experiments (i.e. decrease of activity in inlet reservoir, increase in outlet reservoir, concentration profile in cement layer) after three weeks, it was necessary to use the multicomponent

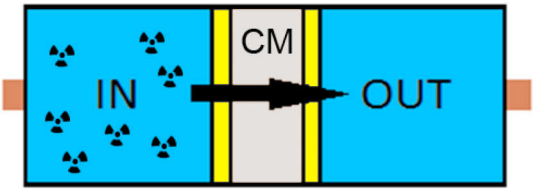

Fig. 1. Schematic of the diffusion cell used for through diffusion experiments (CM: compacted cementitious material, two thin layers: filter).

fitting procedure prepared in the GoldSim environment (described in Baborová et al. (2016)), since steady state was not reached.

3. Results and discussion

3.1. X-ray diffraction analysis

A significant difference between the XRD spectra of concrete, HCP and CSH was observed, as exemplarily shown for the OPC based materials in Fig. 2. A strong signal of quartz from the aggregates in the concrete turned the analysis of concrete CEM I virtually impossible, since the strong peaks of quartz made a lot of other peaks indeterminable, except for major peaks of calcite and portlandite. The spectrum for HCP CEM I shows mainly the new formation of calcium compounds, especially portlandite $Ca(OH)_2$ and calcite $CaCO_3$. However, there is no CSH phase, which has a major peak in the area 29° 2Θ (Zeng et al., 2014), visible in the diffraction pattern of the cementitious materials, due to the stronger lines of other crystalline compounds in comparison to the mainly amorphous or ill-crystalline CSH (Atkins and Glasser, 1992). On the other hand, there are unidentified small peaks in the spectra of C CEM I and HCP CEM I in the areas of 32 and 50° 2Θ, which can be considered as belonging to CSH. Due to the strong signal of calcite in the area of 29° 2Θ, the peak of CSH is obscured and it is not possible to confirm any compound without confirming all peaks in the spectrum. In this case an experimental set-up with higher discrimination could help.

The spectrum of the CSH sample shows the main CSH peaks (29.7°, 32.2° and 50.1° 2Θ) corresponding to the coordinates given in the literature (Baur et al., 2004; Nonat, 2004). However, due to the sensitivity of CSH to CO_2 and the significant moisture content (about 77%) of freshly prepared CSH, the XRD spectrum could be influenced by transformations in the CSH during the measurement that was not maintained under an inert atmosphere.

3.2. Sorption experiments – commercial cements

3.2.1. Sorption of ^{226}Ra and ^{223}Ra

The aim of the sorption experiments on HCP and concretes was to understand the influence of temperature and L/S ratio on Ra and Sr sorption on commercial cement materials used in nuclear waste management. Moreover, the use of the unusual Ra isotope ^{223}Ra (instead of ^{226}Ra) should be evaluated. In Fig. 3, the R_d values obtained from the sorption experiment with isotopes ^{226}Ra and ^{223}Ra on HCP and concrete based on CEM I at room temperature are shown with the trends of these values with L/S ratio indicated. The same comparison was also made for HCP CEM II and C CEM III.

Based on the comparison of the data and trends obtained for the sorption of both isotopes onto commercial cement materials, it can be seen that for HCP CEM I and C CEM I the R_d's in the investigated range of L/S ratios 10–200 L kg^{-1}, are approximately in the same range, but trends in behaviour depending on the L/S ratio differ, as shown for these materials in Fig. 3. The R_d values are in the range 30–170 L kg^{-1} (30–125 L kg^{-1} for ^{226}Ra and 45–170 L kg^{-1} for ^{223}Ra) for the studied L/S ratios. The same conclusions are valid also for other two materials studied. Thus, results obtained using the less-common isotope ^{223}Ra can be used as an estimate of the R_d values of ^{226}Ra within the ranges of L/S ratios used in this study, although the initial Ra concentrations are orders of magnitude different. It is because there is a small difference between these values obtained for ^{223}Ra and ^{226}Ra in contact with cement material according to the t-distribution test at the significance level of $\alpha = 0.05$. What must be pointed out is that the similarity of the values obtained applies only to this L/S range, because the trend clearly identify data obtained with ^{223}Ra will express a sorption isotherm of convex shape whereas R_d's of ^{226}Ra correspond to a sorption isotherm of almost linear or concave shape. Parameters of both isotherm types (Langmuir and Freundlich, for equation see Table 1) are summarized in Table 2. The different behaviour of both isotopes is probably caused by the significantly different initial concentrations of radium ($c_0(^{226}Ra) \approx 5 \cdot 10^{-7}$ mol L^{-1}, $c_0(^{223}Ra) \approx 10^{-12}$ mol L^{-1}). The comparison of HCP's and concretes indicates a small difference in sorption behaviour as the average value of R_d for HCP's is 70 L kg^{-1}, whereas for concretes it is 105 L kg^{-1}. This corresponds to the assumption of higher R_d values in concretes due to the lower C/S ratio caused by the addition of admixtures. However, based on the above mentioned t-distribution test this difference is not statistically significant.

The parameter $K_L < 0$ (accompanied by $Q < 0$) in the Langmuir isotherm and the parameter $p > 1$ in the Freundlich isotherm indicate a convex shape for all ^{223}Ra experimental data, while $K_L > 0$ (and $Q > 0$) and $p < 1$ indicate for most ^{226}Ra data a concave shape of isotherms except for the experiment with HCP CEM I, where K_L is negative (i.e. the isotherm is convex). This effect may be due to the fact that the isotherm is close to linear in this case so that either convex or concave shapes might be fitted with nearly similar goodness of fit. The formal

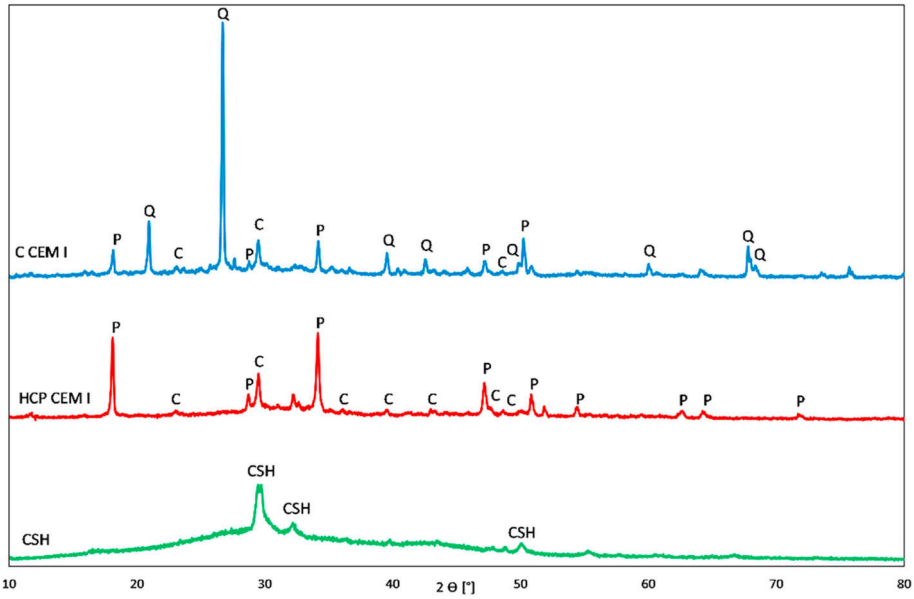

Fig. 2. Comparison of XRD spectra of C CEM I, HCP CEM I and CSH samples (P – Portlandite, C – Calcite, Q – Quartz).

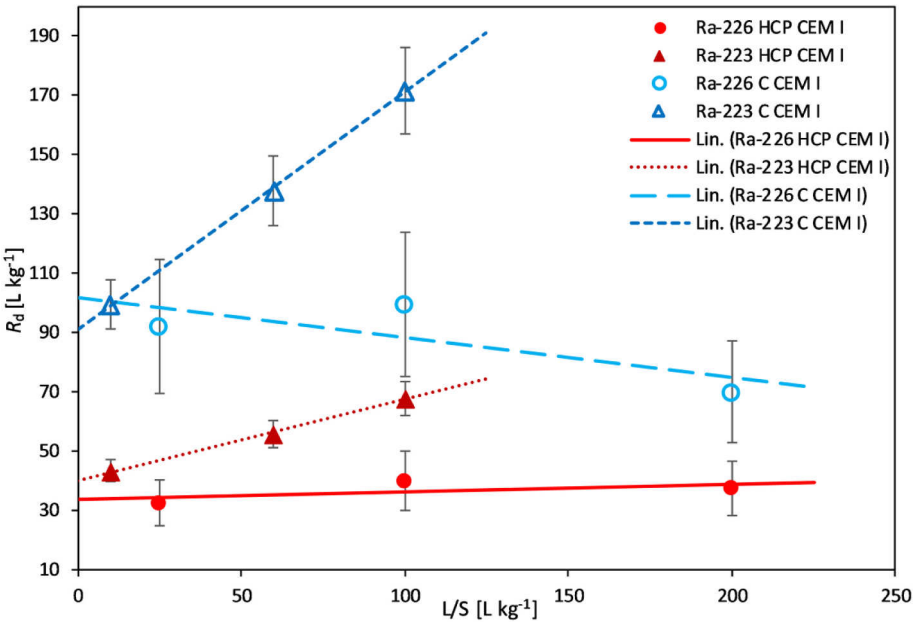

Fig. 3. R_d values of ^{226}Ra and ^{223}Ra on commercial cement materials in cementitious leachate or portlandite water at room conditions as function of L/S ratio with trends of dependences of R_d values on L/S indicated.

Table 2
Parameters of Langmuir and Freundlich isotherms corresponding to dependencies of R_d values on L/S ratios in Fig. 3 and other studied materials. (K_L (L mol^{-1}), Q (mol kg^{-1}), K_F (L kg^{-1})).

	HCP CEM I		HCP CEM II		C CEM I		C CEM III	
	^{223}Ra	^{226}Ra	^{223}Ra	^{226}Ra	^{223}Ra	^{226}Ra	^{223}Ra	^{226}Ra
Langmuir parameters								
Q	$-5.0\cdot10^{-11}$	$-4.7\cdot10^{-5}$	$-7.1\cdot10^{-11}$	$5.9\cdot10^{-5}$	$-6.9\cdot10^{-11}$	$4.3\cdot10^{-5}$	$-3.3\cdot10^{-11}$	$2.4\cdot10^{-5}$
K_L	$-8.9\cdot10^{11}$	$-6.2\cdot10^{5}$	$-9.5\cdot10^{11}$	$2.1\cdot10^{6}$	$-1.6\cdot10^{12}$	$4.0\cdot10^{6}$	$-2.2\cdot10^{12}$	$4.8\cdot10^{7}$
χ^2/df	0.52	1.10	7.60	4.47	0.32	0.93	1.16	0.26
Freundlich parameters								
p	1.39	1.25	1.44	0.80	1.36	0.62	1.72	0.23
K_F	$4.4\cdot10^{6}$	$1.5\cdot10^{3}$	$3.3\cdot10^{7}$	3.8	$6.5\cdot10^{6}$	$2.7\cdot10^{-1}$	$2.5\cdot10^{11}$	$7.0\cdot10^{-4}$
χ^2/df	0.89	1.01	10.49	5.57	0.74	1.27	0.94	0.27

description of experimental sorption isotherms by selected functions (Langmuir and Freundlich) enabled us to evaluate results of sorption kinetic studies by a set of kinetic models (see Table 1).

3.2.2. *Comparison of Ra and Sr sorption*

In previous studies (e.g. Tits et al., 2006b), it has been suggested that ^{90}Sr might be a suitable analogue for the assessment of Ra sorption on cementitious materials. In our case a different Sr isotope (^{85}Sr) was used and directly compared with ^{223}Ra in order to determine the efficiency of

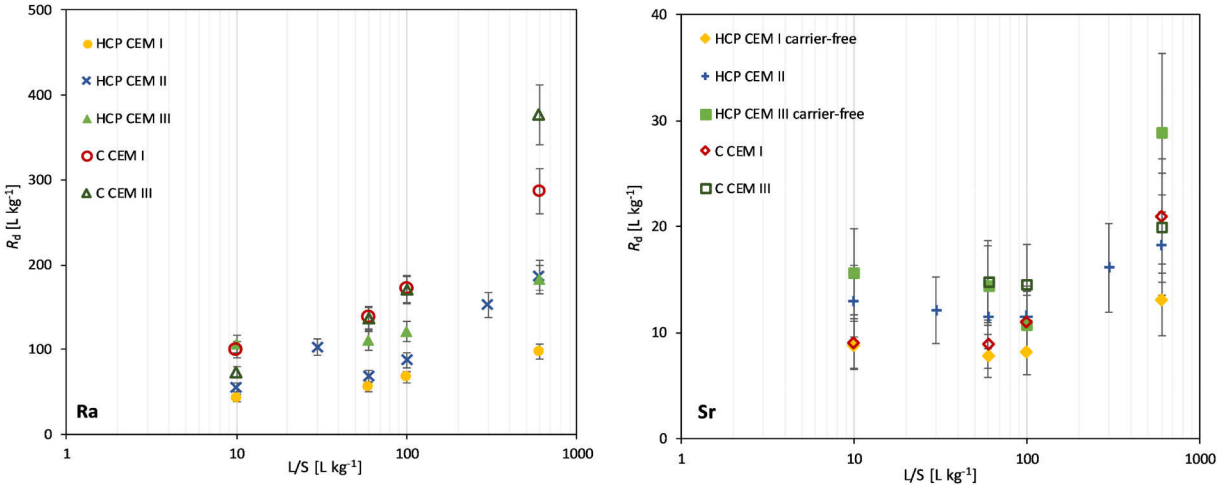

Fig. 4. Comparison of distribution ratio of ^{223}Ra and ^{85}Sr on several commercial cement materials in saturated $Ca(OH)_2$ solution (portlandite water) at 22 °C.

using Sr as an analogue in the case of sorption on cementitious materials and to obtain R_d values for such heterogeneous materials. The comparison of Sr and Ra sorption on HCP and concrete for various experimental conditions is shown in Figs. 4 and 6. Figs. 5 and 7 show the sorption isotherms obtained by fitting the selected experimental data f (q,c) with the Langmuir and Freundlich isotherm models.

When comparing the distribution coefficients of Ra and Sr on cementitious materials, R_d values of Ra are considerably higher (y axis scale is 10 times higher for radium than for strontium in Figs. 4 and 6). Obtained R_d values for Ra uptake are in the range of 50–380 L kg^{-1}, while that for Sr are only 10–30 L kg^{-1}. Both ranges are comparable with previous knowledge as mentioned before for Ra (e.g. Holland and Lee, 1992; Lange et al., 2018; Tits et al., 2006a) and for Sr summarized in e.g. Li and Pang (2014).

The effect of the L/S ratio over all experimental configurations (see Figs. 4 and 6) is much more apparent for Ra, where it is generally possible to say that R_d increases with a higher L/S ratio, which corresponds to a non-linear isotherm of convex type. For Sr, the R_d values in the range of L/S = 10–600 L kg^{-1} can be considered nearly constant, but the isotherms are not linear, the type of them is both convex and concave, which may be due to the proximity of linearity and also to the measurement error. All obtained parameters of both isotherms are in Table 4 (see below).

The convex type of the isotherm for Ra and the nearly linear type (slightly concave in this case) of the isotherm for Sr in the experiments without carrier are demonstrated in Fig. 5. The carrier-free arrangement for Sr was chosen because the conditions (concentration of radionuclide) correspond better to the experiments with Ra.

Fig. 4 (left – ^{223}Ra) shows slightly higher sorption on concretes in comparison with HCP's as mentioned above and also higher sorption on the cements with admixtures (CEM II, CEM III) in comparison to the OPC (CEM I).

Based on the obtained results, it can be concluded that strontium is an insufficient analogue of radium for this type of study, if the aim is to obtain accurate values of distribution ratios.

The reason for the different behaviour of these divalent cations could be due to their different size when hydrated ($Ca^{2+} > Sr^{2+} > Ba^{2+} > Ra^{2+}$) and when sorbed ($Ca^{2+} < Sr^{2+} < Ba^{2+} < Ra^{2+}$) (Cheng et al., 2018; Matsuda and Mori, 2014a, 2014b; Shannon, 1976). In hydrated form, Ra is the smallest of the listed elements and can therefore more easily diffuse into the solid phase.

It must be added that portlandite water as a working solution is merely an approximation to cement water and the cementitious materials were not in equilibrium with the solution during sorption experiments. When studying the evolution of the working solutions during the experiments, it was observed that with decreasing L/S ratio the concentration of Ca in the original portlandite water decreased, while the concentrations of other cations (K, Na, Mg), including Sr, increased. The concentration changes in working solutions were more distinct with increasing temperature. The problematics of leachate composition will be further studied.

3.2.3. Influence of temperature

The effect of temperature on the sorption of ^{223}Ra and ^{85}Sr on HCP CEM II is depicted in Fig. 6, indicating that there is no significant influence of temperature on Sr uptake on this HCP up to 80 °C, since the R_d-values are practically constant over the investigated temperature range within the experimental error. The measured variations were indistinguishable from the statistical fluctuations of the experimental results. At a first glance, the Sr sorption isotherms seem to be close to linear taking into account the error bars of the R_d values. However, a detailed (mathematical) view on the Sr sorption isotherms reveals that the isotherms are of convex type for temperatures of 22 and 50 °C, while the isotherm referring to a temperature of 80 °C is concave, but the difference is only very small due to the proximity to linearity. For ^{223}Ra, the data suggest an increase in R_d values at elevated temperatures; this effect of temperature on ^{223}Ra sorption is more apparent at smaller L/S ratios, e.g. of 10 L kg^{-1}. Therefore, temperature significantly affects the shape of the ^{223}Ra isotherm, which, at a temperature higher than 50 °C changes from convex to concave as shown in Fig. 7. Thus, the change in the shape of the isotherm with increasing temperature is the same for both elements, but due to the evident approach to linearity the uncertainty of shape type is more apparent for Sr.

All R_d values presented within Figs. 4–8 (see below) are summarized in Table 3 and the parameters of the corresponding isotherms are presented in Table 4.

3.2.4. Influence of carrier on Sr sorption

Regarding the uptake of Sr it has to be pointed out that all the cementitious materials used contain stable Sr, which may affect the sorption experiments, since there will be always some Sr present in the liquid phase due to the leaching of the cement materials (in the concentration range of 10^{-4}–10^{-6} mol L^{-1}). In the case of HCP CEM II the exchangeable amount of Sr in the material was determined to be equal to 4.04 mmol kg^{-1}. For C CEM I and C CEM III, the leachable Sr content was about 60% and 30%, respectively, in comparison to HCP CEM II. Even in the case of Ra this is not trivial, since according to Rubáš (2015) the ^{226}Ra concentration in various cements (CEM I, CEM II and CEM III) is in the order of 10^{-12} mol kg^{-1}, which is comparable to the working concentration of ^{223}Ra. However, it was verified here that the ^{226}Ra content in the leachates from HCP CEM I, HCP CEM II and HCP CEM III (L/S 10 L kg^{-1}, after 4 days of contact) was at the background level (gamma

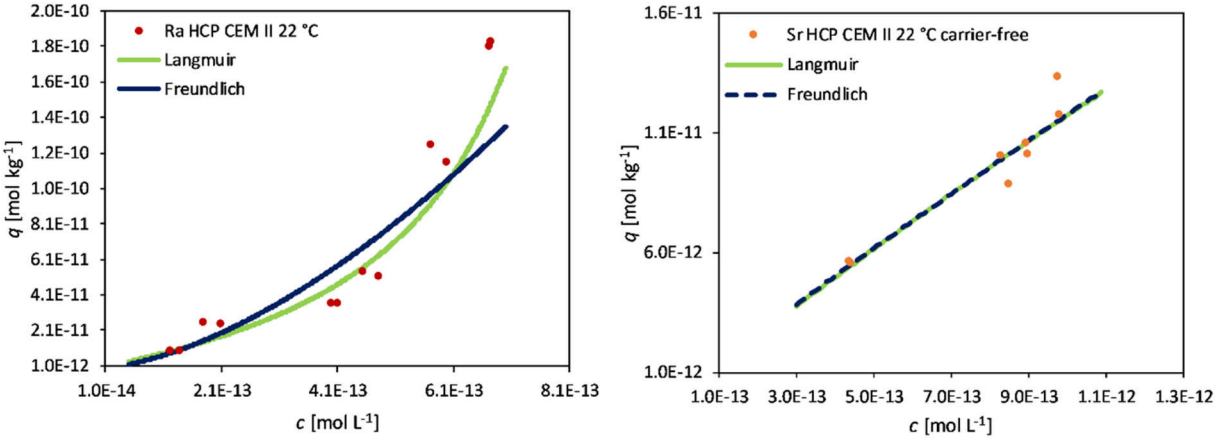

Fig. 5. Sorption isotherms of ^{223}Ra and ^{85}Sr systems selected from the data in Fig. 4 (Ra) and Fig. 8 (Sr, see below). The data points presented in Fig. 4 are shown here in the form of two parallel determinations for demonstrating the uncertainty.

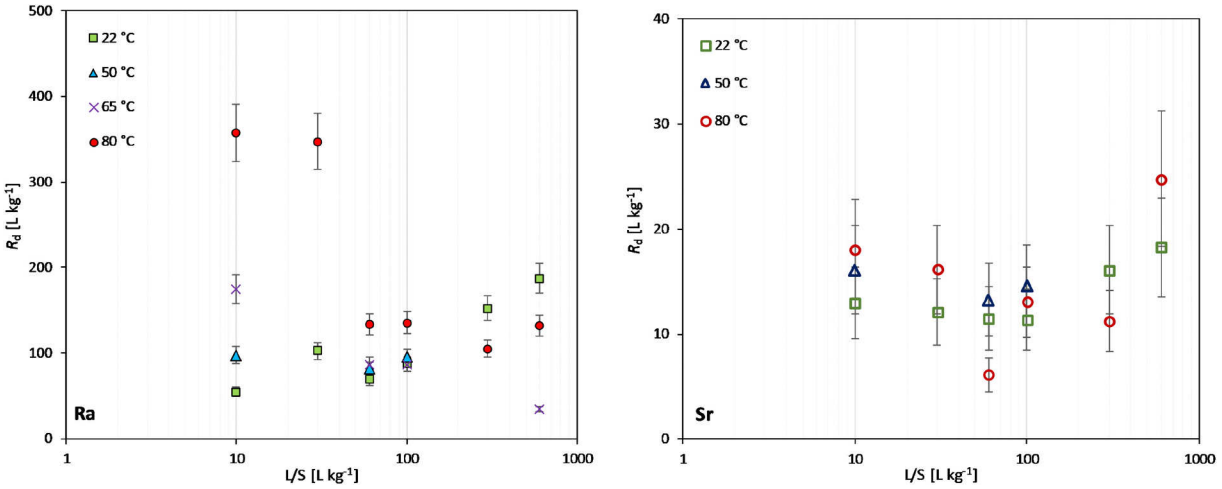

Fig. 6. Comparison of distribution ratios of ^{223}Ra and ^{85}Sr on HCP CEM II in saturated $Ca(OH)_2$ solution (portlandite water) at different temperatures and different L/S ratios.

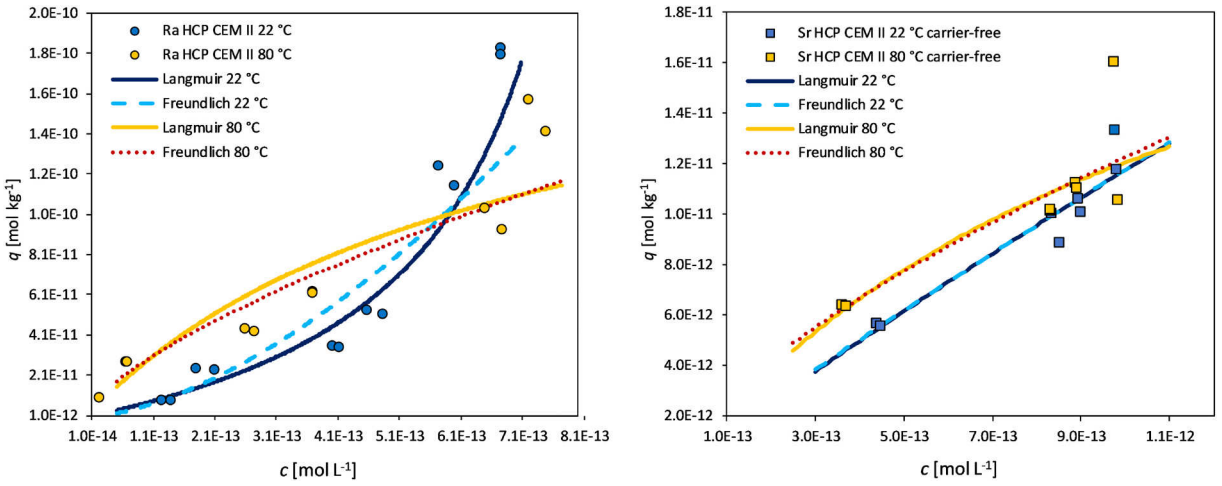

Fig. 7. Sorption isotherms of ^{223}Ra and ^{85}Sr systems selected from the data in Fig. 6 reflecting the influence of change in system temperature. The data points presented in Fig. 6 are shown here in the form of two parallel determinations for demonstrating the uncertainty.

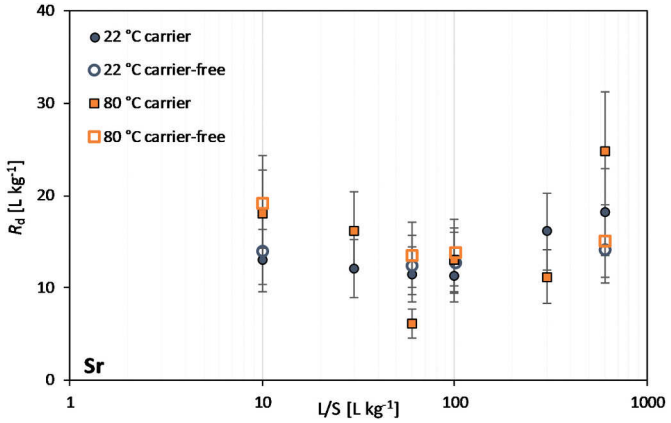

Fig. 8. Influence of carrier ($3.5 \cdot 10^{-4}$ mol L^{-1} $SrCl_2$) on sorption of ^{85}Sr on HCP CEM II in saturated $Ca(OH)_2$ at 22 and 80 °C.

Table 3
R_d values of ^{223}Ra and ^{85}Sr for sorption on commercial cement materials in L/S range of 10–600 L kg^{-1} (* indicates usage of a carrier in the case of Sr (c = $3.5 \cdot 10^{-4}$ mol L^{-1}), the average error of determination is 9.5% for radium and 26% for strontium).

Material	T [°C]	R_d ^{223}Ra [L kg^{-1}]	R_d ^{85}Sr [L kg^{-1}]
HCP CEM I	22	40–100	8–13
HCP CEM III	22	100–180	11–29
C CEM I	22	100–290	9–21*
C CEM III	22	70–380	15–20*
HCP CEM II	22	50–190	11–18*
			12–15
HCP CEM II	50	80–100	13–16*
HCP CEM II	65	30–180	×
HCP CEM II	80	100–360	6–25*
			13–20

Table 4
Parameters of sorption isotherms fitted with Langmuir and Freundlich type relations: ^{223}Ra and ^{85}Sr systems (see Figs. 5 and 7, * indicates usage of a carrier in the case of Sr ($c = 3.5 \cdot 10^{-4}$ mol L^{-1}); (K_L (L mol^{-1}), Q (mol kg^{-1}), K_F (L kg^{-1})).

Ra	HCP CEM II				HCP CEM I	C CEM I	HCP CEM III	C CEM III
	22 °C	50 °C	65 °C	80 °C	22 °C	22 °C	22 °C	22 °C
Langmuir parameters								
Q	$-6.3 \cdot 10^{-11}$	$3.1 \cdot 10^{-9}$	$5.1 \cdot 10^{-11}$	$2.1 \cdot 10^{-10}$	$-4.8 \cdot 10^{-11}$	$-9.2 \cdot 10^{-11}$	$-1.5 \cdot 10^{-10}$	$-5.1 \cdot 10^{-11}$
K_L	$-1.0 \cdot 10^{12}$	$3.7 \cdot 10^{10}$	$8.3 \cdot 10^{12}$	$1.5 \cdot 10^{12}$	$-9.3 \cdot 10^{11}$	$-1.3 \cdot 10^{12}$	$-7.5 \cdot 10^{11}$	$-1.7 \cdot 10^{12}$
χ^2/df	6.83	1.02	9.95	9.08	0.40	1.33	1.77	105.72
Freundlich parameters								
P	1.61	0.98	0.57	0.69	1.63	1.54	1.26	1.97
K_F	$4.7 \cdot 10^{9}$	68	$3.7 \cdot 10^{-4}$	$2.6 \cdot 10^{-2}$	$6.0 \cdot 10^{9}$	$1.2 \cdot 10^{9}$	$2.9 \cdot 10^{5}$	$3.4 \cdot 10^{14}$
χ^2/df	14.39	1.00	9.24	4.59	5.38	3.37	5.19	4.31

Sr	* HCP CEM II			HCP CEM II		HCP CEM I	*C CEM I	HCP CEM III	*C CEM III
	22 °C	50 °C	80 °C	22 °C	80 °C	22 °C	22 °C	22 °C	22 °C
Langmuir parameters									
Q	$-1.3 \cdot 10^{-2}$	$-1.1 \cdot 10^{-2}$	$1.3 \cdot 10^{-2}$	$1.3 \cdot 10^{-10}$	$2.6 \cdot 10^{-11}$	$-2.9 \cdot 10^{-11}$	$-3.4 \cdot 10^{-3}$	$1.3 \cdot 10^{-10}$	$6.5 \cdot 10^{-3}$
K_L	$-7.4 \cdot 10^{2}$	$-1.0 \cdot 10^{3}$	$1.5 \cdot 10^{3}$	$1.0 \cdot 10^{11}$	$8.4 \cdot 10^{11}$	$-2.3 \cdot 10^{11}$	$-1.6 \cdot 10^{3}$	$1.1 \cdot 10^{11}$	$9.5 \cdot 10^{3}$
χ^2/df	3.26	16.64	6.59	0.75	1.61	4.52	8.56	24.46	4.40
Freundlich parameters									
P	1.22	1.43	0.81	0.93	0.67	1.24	1.85	1.11	0.35
K_F	74.6	586	2.98	1.74	$1.2 \cdot 10^{-3}$	$7.1 \cdot 10^{3}$	$1.1 \cdot 10^{4}$	268	$8.6 \cdot 10^{-2}$
χ^2/df	3.57	22.84	7.44	0.73	1.58	4.92	10.89	33.17	3.52

spectrometric determination).

To evaluate the effect of a stable Sr carrier on the uptake of radioactive ^{85}Sr, sorption experiments with HCP CEM II were performed at 22 and 80 °C with and without the addition of a Sr carrier (i.e. $3.5 \cdot 10^{-4}$ mol L^{-1} $SrCl_2$); the results are shown in Fig. 8. From Fig. 8 it is evident that there is no significant effect of the use of a given Sr carrier concentration on the distribution ratios, especially in the L/S range of 10–100 L kg^{-1}.

3.3. Sorption experiments – CSH

In Fig. 9. R_d values for the uptake of ^{226}Ra and ^{90}Sr on CSH (C/S ratio = 1.4) are shown as a function of solution concentration. The comparison confirms significantly higher R_d values of Ra sorption with the range of thousands L kg^{-1} (average 1981 ± 383 L kg^{-1}) and R_d values of Sr sorption at about 10^2 L kg^{-1} (108 ± 7 L kg^{-1}). In the investigated concentration range, both elements reveal linear sorption isotherms. Sorption on CSH is considerably higher than that on the commercial cement materials (cf. Lange et al. (2018)), especially for Ra, where the R_d's for the cementitious materials used in our study are in range of 50–380 L kg^{-1} for Ra and in range of 10–30 L kg^{-1} for Sr, as shown above.

Sorption experiments with Ra in the scientific literature are quite rare, but values obtained in this paper are in good agreement with the range of distribution ratios for Ra on the pure CSH phases which were determined to be in the order of 10^2–10^4 L kg^{-1} (Lange et al., 2018; Olmeda et al., 2019; Tits et al., 2006a). An average R_d value of CSH with C/S = 1.4 is reported as (1805 ± 722) L kg^{-1} in Lange et al. (2018).

As can be deduced from data presented in Fig. 9, sorption isotherms are practically linear in both cases and the pure CSH has different sorption properties than cementitious materials described above.

According to e.g. Tits et al. (2006a) and Wieland et al. (2008) Ra and Sr sorption on CSH phases, but also on HCP's, is a linear and reversible process, that is probably governed by cation exchange of Ra^{2+} or Sr^{2+} vs.

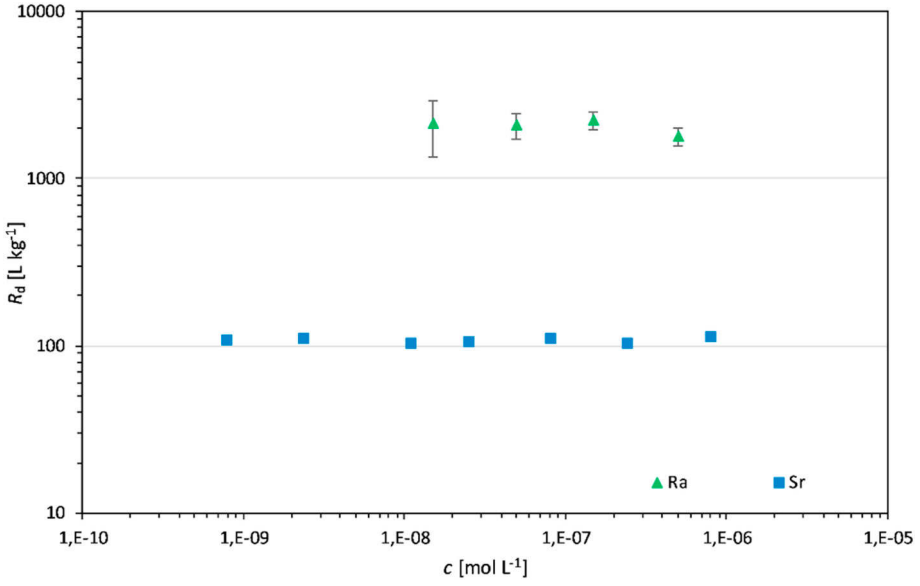

Fig. 9. Comparison of distribution ratios, R_d, of ^{226}Ra and ^{90}Sr sorption on CSH with C/S 1.4 (for Sr the error corresponds to the size of the data points) as a function of their aqueous concentration.

Ca^{2+} on the edge and planar silanol groups of the CSH phases, which are deprotonated under the alkaline conditions of cement systems, the negative charge carried by deprotonated silanol groups is neutralized e.g. by Ca and the exchange goes as described for Ra in Eq. (4) (the process is analogous for Sr):

$$Ca\text{-}CSH + Ra^{2+} \Longleftrightarrow Ra\text{-}CSH + Ca^{2+} \quad (4)$$

There is a question, what ionic forms of the alkaline earth metals, especially Ra, are present under the given conditions in the liquid phase. For this purpose, speciation calculations were performed. Because the composition of the used solutions is not known exactly, the obtained dependencies should be considered as indicative, however useful. Regarding the forms of Ra upon sorption on CSH, here, given the conditions mentioned above (practically CO_2-free), these are clearly the cationic forms of Ra^{2+} and $RaOH^+$. In the case of experiments with other cementitious materials, due to the presence of carbonates and sulphates, this is not so clear. As an example, a simulated pore water containing a saturated solution of portlandite ($Ca(OH)_2$), and further components leached out of the cementitious materials, i.e. Na^+, K^+, Ca^{2+}, SO_4^{2-}, Cl^-, OH^- etc. (electroneutrality must apply) was used for the calculations. The concentration of these components is in units of up to tens of millimoles per litre, while the initial concentration of ^{223}Ra was set to $1{\cdot}10^{-12}$ mol L^{-1}. The speciation of Ra was calculated as a function of pH, in the range of pH 5–14, and with access of atmospheric CO_2. The results are shown in Fig. 10.

The calculations, which are rather conservative, show that in the systems studied, the dissolved radium, and similarly other alkaline earth metals, is mainly present in form of cationic species (Ra^{2+}, $RaOH^+$ and $RaHCO_3^+$) and uncharged aqueous complexes such as $RaCO_3^0$(aq) and $RaSO_4^0$(aq). It seems that the mechanism of sorption is mainly the capture of cations (in particular Ra^{2+}) via exchange on deprotonated silanol groups. The dissolved cationic forms of radium, such as Ra^{2+}, are in thermodynamic equilibrium with its other aqueous species such as Ra-carbonato and Ra-sulphato complexes. Thus, when Ra^{2+} is drawn from the system by sorption onto the cementitious materials, the complexes dissociate to re-establish equilibrium and virtually full sorption of Ra^{2+} can take place.

3.4. Kinetic models for two-phase (liquid-solid) systems

Results of kinetic experiments of ^{223}Ra sorption in several system configurations are presented in Fig. 11; it is apparent from the close-to-zero concentration changes that a close-to-equilibrium state was reached after approximately 30–40 h, except for the system C CEM III, L/S = 100 that required at least 96 h.

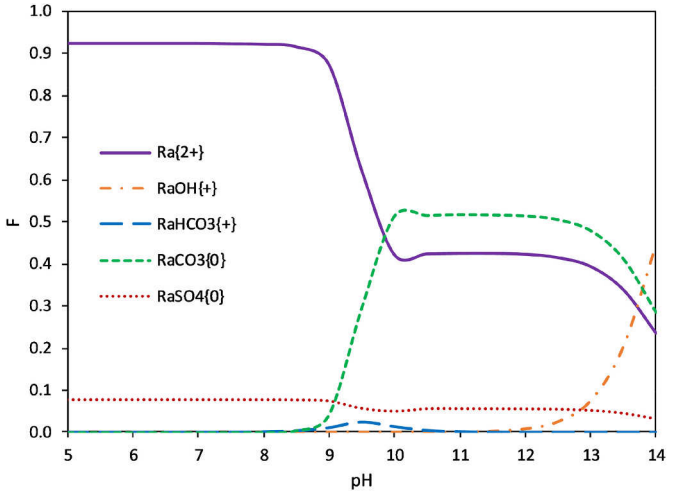

Fig. 10. Estimation of radium speciation in liquid phase of studied cement experiments (F refers to fraction).

The kinetic models presented in Table 1 were exemplarily applied to 7 sets of kinetic data on the Ra uptake on three types of cementitious materials under various experimental conditions. Moreover, an experiment with ^{85}Sr (with carrier $SrCl_2$) was evaluated for comparison (this experiment was performed using a HCP leachate instead of saturated Ca $(OH)_2$). A special case of the Freundlich model ($p = 1$, corresponding to the so-called linear K_d-model) and the Langmuir model were initially used to describe the sorption isotherms. The results obtained using both models are, on the basis of *WSOS/DF* values, applicable, however, due to the frequently observed non-linearity of the isotherm, the Langmuir model was preferred for the presentation of the results.

The $\frac{\chi 2}{\nu}$ (*WSOS/DF*) values derived for the FD, DM, ID and CR kinetic models (cf. Table 1) to describe the kinetics of Ra and Sr uptake in the selected systems are given in Table 5. A meaningful value of $\frac{\chi 2}{\nu}$ must meet the requirement $0.1 < \frac{WSOS}{DF} < 20$ according to (Herbelin and Westall, 1996), but it is preferred to be as low as possible or at least less than 10. When interpreting the sorption data using the Freundlich (K_d-model), the DM or FD model were the most suitable for the description of the Ra sorption kinetics. However, with the use of the Langmuir sorption model, the film diffusion (FD model) emerged as superior. For Sr, in both cases the ID model was found to be the most suitable.

The difference between both radionuclides can be attributed to the very different concentration levels ($^{223}Ra \approx 10^{-12}$ mol L^{-1}, Sr $3.5{\cdot}10^{-4}$ mol L^{-1}) used in the experiments, where the lower concentration corresponds to FD (film diffusion model) or DM (two-film model) and the higher to ID (diffusion in inert layer). This phenomenon is due to the fact that the concentration of the sorbing component is one of the parameters determining the control process during sorption via the ion exchange mechanism. At lower concentrations the slowest event and thus the control process is film diffusion, whereas at higher concentrations it is diffusion in an inert layer (ID model) (Helfferich, 1959).

It can be seen from results in Table 5 that the choice of the "ideal" kinetic model is not unambiguous. However, this quantitative analysis can help to evaluate the sorption properties of cementitious materials and eventually to help for further development of transport models for Ra in cementitious barriers.

Evaluation of kinetic data (sorption of ^{223}Ra onto HCP CEM II) at two temperatures (22 and 80 °C) and two L/S ratios (L/S 10 and 100 L kg^{-1}) were used to determine values of the apparent activation energy, E_A, of the uptake process. Despite the fact that the DM model and the FD model were evaluated as best describing these systems on the basis of *WSOS/DF* (see Table 5), it was not possible to use the kinetic coefficients obtained from these models for the evaluation of E_A. The kinetic coefficients from the CR model for L/S = 10 L kg^{-1} and the ID model for L/S = 100 L kg^{-1} proved to be the most convenient for this purpose. The corresponding values of the total mass transfer coefficients, K_{CR} or K_{ID}, were used to calculate E_A, using Eq. (5), which can be derived by adjusting the Arrhenius equation (Arrhenius, 1889; Levenspiel, 1962), provided that the kinetic coefficients, $K_{CR\text{-}1}$ and $K_{CR\text{-}2}$ or $K_{ID\text{-}1}$ and $K_{ID\text{-}2}$, for two temperatures, T_1 and T_2, respectively, are known. For example, for the CR model, Eq. (5) can be written as

$$E_A = R \cdot \frac{\ln(K_{CR-2}/K_{CR-1})}{{}^1/_{T_1} - {}^1/_{T_2}} \quad (5)$$

where R is gas constant (8.314 J mol^{-1} K^{-1}), $T_1 = 295$ K (22 °C), $T_2 = 353$ K (80 °C), and the coefficients are $K_{CR\text{-}1} = 14.8$ min^{-1} (22 °C), $K_{CR\text{-}2} = 37.0$ min^{-1} (80 °C) for L/S = 10 L kg^{-1} and $K_{ID\text{-}1} = 2.13$ min^{-1} (22 °C), $K_{ID\text{-}2} = 10.0$ min^{-1} (80 °C) for L/S = 100 L kg^{-1}.

Substituting into Eq. (5), we obtain the following values of the apparent activation energies: $E_{A10} = 13.7$ kJ mol^{-1} K^{-1} for L/S = 10 L kg^{-1} and $E_{A100} = 23.1$ kJ mol^{-1} K^{-1} for L/S = 100 L kg^{-1}.

On the basis of these values, it is not possible to clearly identify the

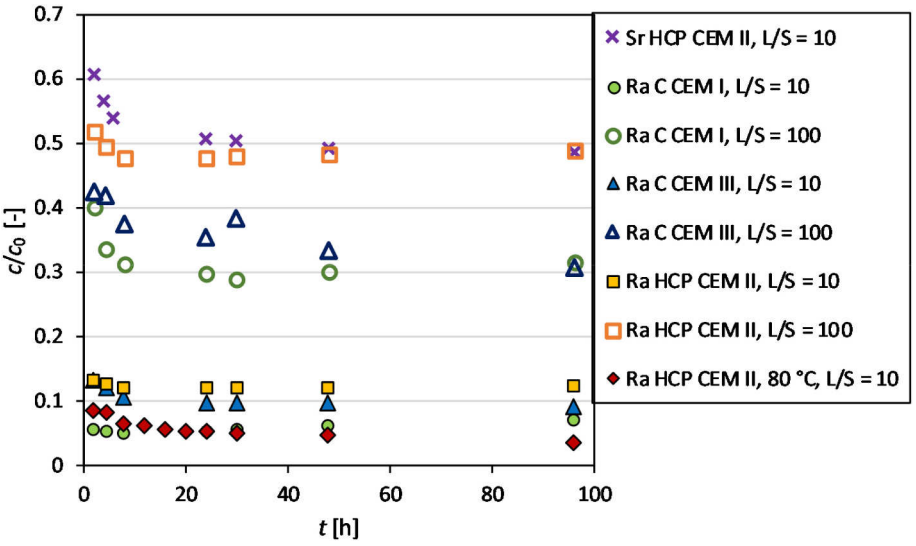

Fig. 11. Sorption kinetics of ^{223}Ra and ^{85}Sr on cementitious materials in saturated $Ca(OH)_2$ working solution at 22 and 80 °C and L/S 10 and 100 L kg^{-1}. Error bars are omitted for the sake of clarity.

Table 5

The $\frac{\chi 2}{\nu}$ (WSOS/DF) values obtained by evaluation of the kinetics of Ra and Sr sorption in several systems for various phase ratios L/S and two working temperatures using different kinetic models (cf. Table 1; best fits shown in bold; the Langmuir model was used for the description of sorption isotherms).

Experiment	Isotherm K_L:[L mol^{-1}] Q:[mol kg^{-1}]	L/S [L kg^{-1}]	*χ2/ν (WSOS/DF)*			
			FD	DM	ID	CR
Ra, HCP CEM II, 22 °C, Ca(OH)$_2$	$Q = -3.08 \cdot 10^{-11}$ $K_L = -1.68 \cdot 10^{12}$	10	**8.41**	9.36	13.30	11.0
		100	**0.46**	0.65	2.89	2.08
Ra, HCP CEM II, 80 °C, Ca(OH)$_2$	$Q = 8.50 \cdot 10^{-10}$ $K_L = 2.77 \cdot 10^{11}$	10	190	**10.10**	52.2	212
		100	5.97	**3.94**	4.10	4.13
Ra, C CEM I, 22 °C, Ca(OH)$_2$	$Q = -1.89 \cdot 10^{-10}$ $K_L = -6.41 \cdot 10^{11}$	10	**20.5**	492	61.0	57.0
		100	**3.20**	3.62	294	9.20
Ra, C CEM III, 22 °C, Ca(OH)$_2$	$Q = -3.23 \cdot 10^{-11}$ $K_L = -2.86 \cdot 10^{-12}$	10	**0.41**	86.8	×	×
		100	**2.15**	253	198	204
Sr, HCP CEM II, 22 °C, leachate	$Q = 7.71 \cdot 10^{-3}$ $K_L = 3.67 \cdot 10^{-3}$	10	6.97	5.97	**2.18**	5.14

rate-controlling process of the sorption studied (diffusion or chemical reaction), as a general rule of thumb, the boundary value of apparent activation energy dividing diffusion and chemical reaction processes ranges from ca. 20–40 kJ mol^{-1}. Values below this interval suggest diffusion as the rate-controlling process, while it is the chemical reaction for higher values. This unclear behaviour corresponds to the possibility to fit different kinetic models (cf. Table 1) with similar *WSOS/DF*, which take into account different rate-controlling processes.

3.5. Diffusion experiments with ^{223}Ra and ^{85}Sr

In addition to the batch sorption experiments, the through diffusion of ^{223}Ra and ^{85}Sr through a compacted layer of crushed HCP CEM II was investigated. The experimental results of Ra and Sr diffusion and corresponding GoldSim model curves are presented in Fig. 12. In this figure, the concentration of both radionuclides in the layer of cementitious material after the termination of the diffusion experiment after three weeks and the evolution of the radionuclide concentrations in the inlet and outlet reservoirs during the experiment are presented. The behaviour of both elements confirmed the assumption that the diffusive transport of Ra would be more retarded than the transport of Sr, due to the stronger radium uptake by HCP. Thus, the observed concentration decrease in the inlet reservoir is more pronounced for Ra as the mass flow into the layer of crushed cementitious material is enhanced by the sorption that causes a stronger concentration gradient close to the boundary filter – cement. The comparison of the activity profiles of Ra and Sr in the cementitious material after the termination of the experiments indicates that neither Sr nor Ra reached steady state within three weeks and depicts the higher uptake of radium on the solids. Corresponding to the shape of the Ra profile in the cementitious material, no Ra was detected in the outlet reservoir.

The diffusion experiment could not be prolonged due to the short half-life of the ^{223}Ra (11.43 days), as the decrease in activity by radioactive decay could affect the measurement, or make it completely impossible.

The quality of fits of the GoldSim model demonstrates that the conceptual model assuming the linearity of the sorption model and reversibility of the sorption process is valid for the retarded diffusive transport of Ra and Sr in the compacted HCP material.

The results of the through diffusion experiments are in agreement with the findings from the batch sorption experiments, as the R_d values determined in the diffusion experiments were about 9 L kg^{-1} for Sr and 150 L kg^{-1} for Ra. Based on the comparison of the dry sample weight with the sum of the weights of the dried cut slices produced at the end of the diffusion experiment, the L/S ratio in the diffusion experiments was about 0.3 L kg^{-1}.

4. Conclusions

Distribution ratios, R_d, of Ra uptake on commercial cement materials that are used or will be used in nuclear waste management in the Czech Republic are in the range of 50–380 L kg^{-1}, while those for Sr were found to be 10–30 L kg^{-1}, both ranges are in agreement to published data. Distribution ratios of Sr were generally constant over the range of L/S ratios from 10 to 600 L kg^{-1}, whereas those for Ra were generally increasing with increasing L/S ratio. The influence of increasing temperature was convincingly recorded only for the sorption of Ra, in particular at lower L/S ratios, leading to an increase in Ra uptake at elevated temperature. Sorption isotherms of Ra and Sr on HCP and

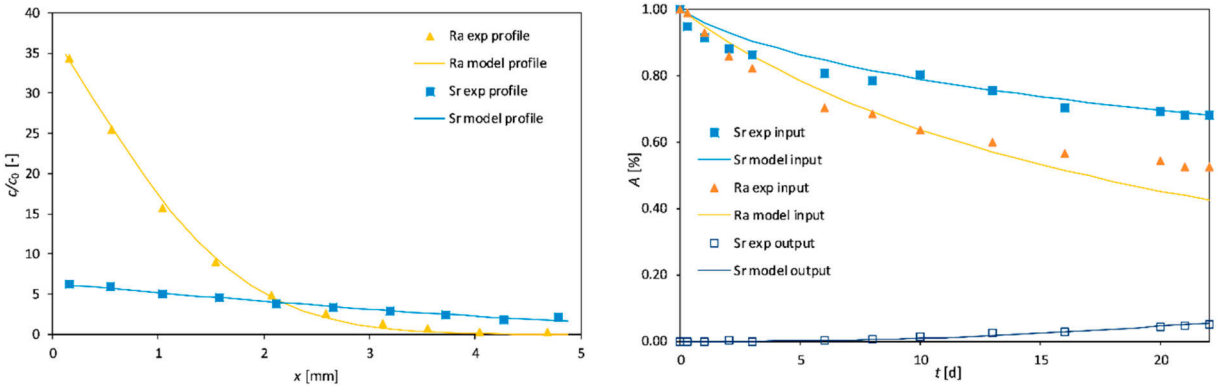

Fig. 12. Results of ^{223}Ra and ^{85}Sr through diffusion experiments in the layer of crushed HCP CEM II in the environment of saturated $Ca(OH)_2$; concentration profile of the sorbed element in the cementitious material (left) and concentrations in the input and output reservoirs respectively (right) are shown with the curves corresponding to the GoldSim model.

concrete were determined; the isotherms of ^{223}Ra are mostly of convex shape, but with elevated temperature the shape changes to concave. Sr isotherms are close to linear in shape. Sorption experiments with a synthesised CSH phase confirmed i) the dominant role of CSH for sorption of alkaline earth metals in cementitious materials, and ii) the significant difference between the uptake of Ra and Sr, with the R_d values decreasing by about an order of magnitude from Ra to Sr, as expected. The experimental data confirmed that the sorption of Sr on cementitious materials is much weaker than Ra sorption and probably has a different dependency on temperature, which renders Sr not suitable as a meaningful analogue for Ra in studies on the performance of cementitious materials in nuclear waste repositories.

It was proved that in the investigated range of L/S ratios (10–200 L kg^{-1}) the R_d values for both Ra isotopes (^{223}Ra and ^{226}Ra) are comparable, although different trends on L/S ratios were observed (convex isotherms for ^{223}Ra and concave for ^{226}Ra), probably caused by the different concentration levels of the Ra isotopes in the experiments.

The kinetics of Sr and Ra uptake by cementitious materials was successfully evaluated by a set of models describing the sorption in heterogeneous systems based on different rate-controlling processes. The FD (film diffusion) model in the case of Ra, and the ID (diffusion in inert layer) model in the case of Sr proved to be the most convenient. The determined values of apparent activation energies did not clearly indicate the rate-controlling process behind the sorption.

R_d values determined by the evaluation of through diffusion experiments with HCP were around 9 L kg^{-1} for Sr, and 150 L kg^{-1} for Ra, in good agreement to the batch sorption data. The concept of these diffusion experiments has been used to work with a significantly smaller but more realistic L/S ratio for the evaluation of the performance of cementitious barriers in a repository that would be difficult to realize in batch experiments. However, the agreement between the different approaches suggest that the data obtained in the batch experiments can be transferred to the diffusive transport in a cementitious barrier system.

Declaration of competing interest

The authors declare that they have no known competing financial interests or personal relationships that could have appeared to influence the work reported in this paper.

Acknowledgement

The research leading to these results has received funding from the European Union's Horizon 2020 Research and Training Programme of the European Atomic Energy Community (EURATOM) (H2020-NFRP-2014/2015) under grant agreement n° 662147 (CEBAMA). Jana Kittnerová acknowledges the opportunity for her research stay at Forschungszentrum Jülich enabled by a CEBAMA mobility measure. This contribution is also partially result of the Radioactive Waste Repository Authority project "Research support for Safety Evaluation of Deep Geological Repository" and partially a result of European Regional Development Fund-Project "Center for Advanced Applied Science" (Grant No. CZ.02.1.01/0.0/0.0/16_019/0000778).

References

Arrhenius, S., 1889. Z. Phys. Chem. 4, 226.
Atkins, M., Glasser, F.P., 1992. Application of Portland cement-based materials to radioactive waste immobilization. Waste Manag. 12, 105–131.
Atkins, M., Glasser, F.P., Kindness, A., 1992. Cement hydrate phases: solubility at 25 °C. Cement Concr. Res. 22, 241–246.
Baborová, L., Vopálka, D., Hofmanová, E., Vetešník, A., 2016. Migration behaviour of strontium in Czech bentonite clay. J. Sustain. Dev. Energy, Water Environ. Syst. 4, 293–306. https://doi.org/10.13044/j.sdewes.2016.04.0023.
Baur, I., Keller, P., Mavrocordatos, D., Wehrli, B., Johnson, C.A., 2004. Dissolution-precipitation behaviour of ettringite, monosulfate, and calcium silicate hydrate. Cem. Concr. Res. 34, 341–348. https://doi.org/10.1016/j.cemconres.2003.08.016.
Bayliss, S., Ewart, F.T., Howse, R.M., Lane, S.A., Pilkington, N.J., Smith-Briggs, J.L., Williams, S.J., 1989. The solubility and sorption of radium and tin in a cementitious near-field environment. Mater. Res. Soc. Symp. Proc. 127, 879–885.
Beneš, P., Štamberg, K., Štegman, R., 1994. Study of the kinetics of the interaction of Cs-137 and Sr-85 with soils using a batch method: methodological problems. Radiochim. Acta 66 (67), 315–321. https://doi.org/10.1524/ract.1994.6667.special-issue.315.
Berner, U., 2003. Project Opalinus Clay: radionuclide concentration limits in the cementitious near-field of an ILW repository. PSI Bericht Nr 2–26, 62.
Brendler, V., 2006. RES3T - Rossendorf Expert System for Surface and Sorption Thermodynamics. Forschungszentrum Rossendorf e.V., Institut of Radiochemistry, Dresden, Germany. https://www.hzdr.de/db/res3t.login.
Chen, J.J., Thomas, J.J., Taylor, H.F.W., Jennings, H.M., 2004. Solubility and structure of calcium silicate hydrate. Cement Concr. Res. 34, 1499–1519. https://doi.org/10.1016/j.cemconres.2004.04.034.
Cheng, W., Liu, C., Tong, T., Epsztein, R., Sun, M., Verduzco, R., Ma, J., Elimelech, M., 2018. Selective removal of divalent cations by polyelectrolyte multilayer nanofiltration membrane: role of polyelectrolyte charge, ion size, and ionic strength. J. Membr. Sci. 559, 98–106. https://doi.org/10.1016/j.memsci.2018.04.052.
Collins, S.M., Pearce, A.K., Ferreira, K.M., Fenwick, A.J., Regan, P.H., Keightley, J.D., 2015. Direct measurement of the half-life of ^{223}Ra. Appl. Radiat. Isot. 99, 46–53. https://doi.org/10.1016/j.apradiso.2015.02.003.
Distler, P., Štamberg, K., John, J., Harwood, L.M., Lewis, F.W., 2020. Thermodynamic parameters of Am(III), Cm(III) and Eu(III) extraction by $CyMe_4$-BTPhen in cyclohexanone from HNO_3 solutions. J. Chem. Thermodyn. 141 https://doi.org/10.1016/j.jct.2019.105955.
Distler, P., Štamberg, K., John, J., Harwood, L.M., Lewis, F.W., 2018. Modelling of the Am(III)–Cm(III) kinetic separation effect observed during metal ion extraction by bis-(1,2,4)-triazine ligands. Separ. Sci. Technol. 53, 277–285. https://doi.org/10.1080/01496395.2017.1384017.
Evans, N.D.M., 2008. Binding mechanisms of radionuclides to cement. Cement Concr. Res. 38, 543–553. https://doi.org/10.1016/j.cemconres.2007.11.004.
Gondolli, J., Večerník, P., 2014. The uncertainties associated with the application of through-diffusion, the steady-state method: a case study of strontium diffusion. Geol. Soc. London, Spec. Publ. 400, 603–612. https://doi.org/10.1144/SP400.3.
Helfferich, F., 1959. Ionenaustauscher, Band I: Grundlagen. Struktur - Herstellung - Theorie. Verlag Chemie GmbH, Weinheim/Bergstraße.

Herbelin, A.L., Westall, J.C., 1996. FITEQL-A Computer Program for Determination of Chemical Equilibrium Constants from Experimental Data. Department of Chemistry, Oregon State University, Corvallis, Oregon. Version 3.2, Report 96-01.

Holland, T.R., Lee, D.J., 1992. Radionuclide getters in cement. Cement Concr. Res. 22, 247–258.

Iwaida, T., Nagasaki, S., Tanaka, S., 2000. Sorption study of strontium onto hydrated cement phases using a sequential desorption method. Radiochim. Acta 88, 463–486.

Jantzen, C., Johnson, A., Read, D., Stegemann, J.A., 2010. Cement in waste management. Adv. Cement Res. 22, 225–231. https://doi.org/10.1680/adcr.2010.22.4.225.

Kozempel, J., Vlk, M., Málková, E., Bajzíková, A., Bárta, J., Santos-Oliveira, R., Malta Rossi, A., 2015. Prospective carriers of ^{223}Ra for targeted alpha particle therapy. J. Radioanal. Nucl. Chem. 304, 443–447. https://doi.org/10.1007/s10967-014-3615-y.

Lagerblad, B., 2001. Leaching Performance of Concrete Based on Studies of Samples from Old Concrete Constructions, p. 85. SKB Technical Report 01-27.

Lange, S., Kowalski, P.M., Pšenička, M., Klinkenberg, M., Rohmen, S., Bosbach, D., Deissmann, G., 2018. Uptake of ^{226}Ra in cementitious systems: a complementary solution chemistry and atomistic simulation study. Appl. Geochem. 96, 204–216. https://doi.org/10.1016/j.apgeochem.2018.06.015.

Levenspiel, O., 1962. Chemical Reaction Engineering, an Introduction to the Design of Chemical Reactors. John Wiley & Sohns, Inc., New York.

Li, K., Pang, X., 2014. Sorption of radionuclides by cement-based barrier materials. Cement Concr. Res. 65, 52–57. https://doi.org/10.1016/j.cemconres.2014.07.013.

Lujaniene, G., Beneš, P., Štamberg, K., Ščiglo, T., 2012. Kinetics of plutonium and americium sorption to natural clay. J. Environ. Radioact. 108, 41–49. https://doi.org/10.1016/j.jenvrad.2011.07.012.

Lützenkirchen, J. (Ed.), 2006. Surface Complexation Modeling. Academic Press, Elsevier Ltd., London.

Matsuda, A., Mori, H., 2014a. A quantum chemical study on hydration of Ra (II): comparison with the other hydrated divalent alkaline earth metal ions. J. Comput. Chem. Japan 13, 105–113. https://doi.org/10.2477/jccj.2013-0011.

Matsuda, A., Mori, H., 2014b. Theoretical study on the hydration structure of divalent radium ion using fragment molecular orbital-molecular dynamics (FMO-MD) simulation. J. Solut. Chem. 43, 1669–1675. https://doi.org/10.1007/s10953-014-0235-7.

Nonat, A., 2004. The structure and stoichiometry of C-S-H. Cem. Concr. Res. 34, 1521–1528. https://doi.org/10.1016/j.cemconres.2004.04.035.

Ochs, M., Mallants, D., Wang, L., 2016. Radionuclide and Metal Sorption on Cement and Concrete, Topics in Safety, Risk, Reliability and Quality. Springer International Publishing, Cham. https://doi.org/10.1007/978-3-319-23651-3.

Olmeda, J., Missana, T., Grandia, F., Grivé, M., García-Gutiérrez, M., Mingarro, M., Alonso, U., Colàs, E., Henocq, P., Munier, I., Robinet, J.C., 2019. Radium retention by blended cement pastes and pure phases (C-S-H and C-A-S-H gels): experimental assessment and modelling exercises. Appl. Geochem. 105, 45–54. https://doi.org/10.1016/j.apgeochem.2019.04.004.

Piqué, À., Arcos, D., Grandia, F., Molinero, J., Duro, L., Berglund, S., 2013. Conceptual and numerical modeling of radionuclide transport and retention in near-surface systems. Ambio 42, 476–487. https://doi.org/10.1007/s13280-013-0399-1.

Richardson, I.G., 2008. The calcium silicate hydrates. Cement Concr. Res. 38, 137–158. https://doi.org/10.1016/j.cemconres.2007.11.005.

Rubáš, P., 2015. Protocol on Measurement and Evaluation of Natural Radionuclide Content in Building Materials (In Czech). Technical and testing building institute, Prague.

Shannon, R.D., 1976. Revised effective ionic radii and systematic studies of interatomic distances in halides and chalcogenides. Acta Crystallogr. A 32, 751–767. https://doi.org/10.1107/S0567739476001551.

SKB, 2011. Long-term Safety for the Final Repository for Spent Nuclear Fuel at Forsmark. Main Report of the SR-Site Project. SKB TR-11-01, p. 271.

Štamberg, K., Cabicar, J., 1980. Models of sorption kinetics in liquid-solid phase systems (in Czech). Acta Polytech. - Tech. Univ. Prague 8, 107–130.

Tits, J., Iijima, K., Wieland, E., Kamei, G., 2006a. The uptake of radium by calcium silicate hydrates and hardened cement paste. Radiochim. Acta 94, 637–643. https://doi.org/10.1524/ract.2006.94.9-11.637.

Tits, J., Wieland, E., Müller, C.J., Landesman, C., Bradbury, M.H., 2006b. Strontium binding by calcium silicate hydrates. J. Colloid Interface Sci. 300, 78–87. https://doi.org/10.1016/j.jcis.2006.03.043.

Treybal, R.E., 1956. Mass Transfer Operations. McGraw-Hill, Book Company, New York.

Wieland, E., Tits, J., Kunz, D., Dähn, R., 2008. Strontium uptake by cementitious materials. Environ. Sci. Technol. 42, 403–409. https://doi.org/10.1021/es071227y.

Zeng, L., Yang, L., Wang, S., Yang, K., 2014. Synthesis and characterization of different crystalline calcium silicate hydrate: application for the removal of aflatoxin B1 from aqueous solution. J. Nanomater. 1–10. https://doi.org/10.1155/2014/431925, 2014.